



Laser Interferometer Space Antenna (LISA)

Time-Delay Interferometry for LISA

Massimo Tinto

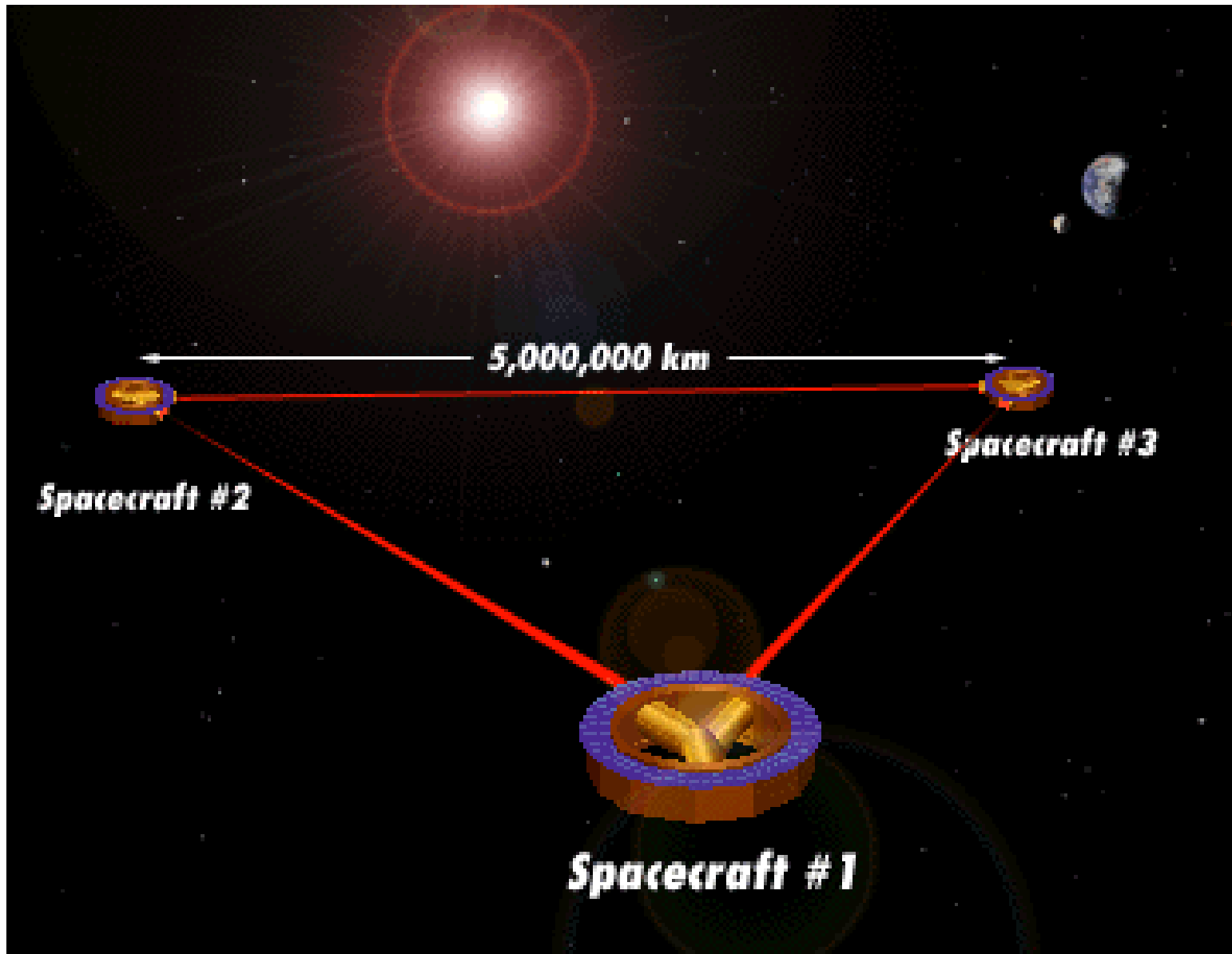
In collaboration with **John Armstrong** and **Frank Estabrook @ JPL**

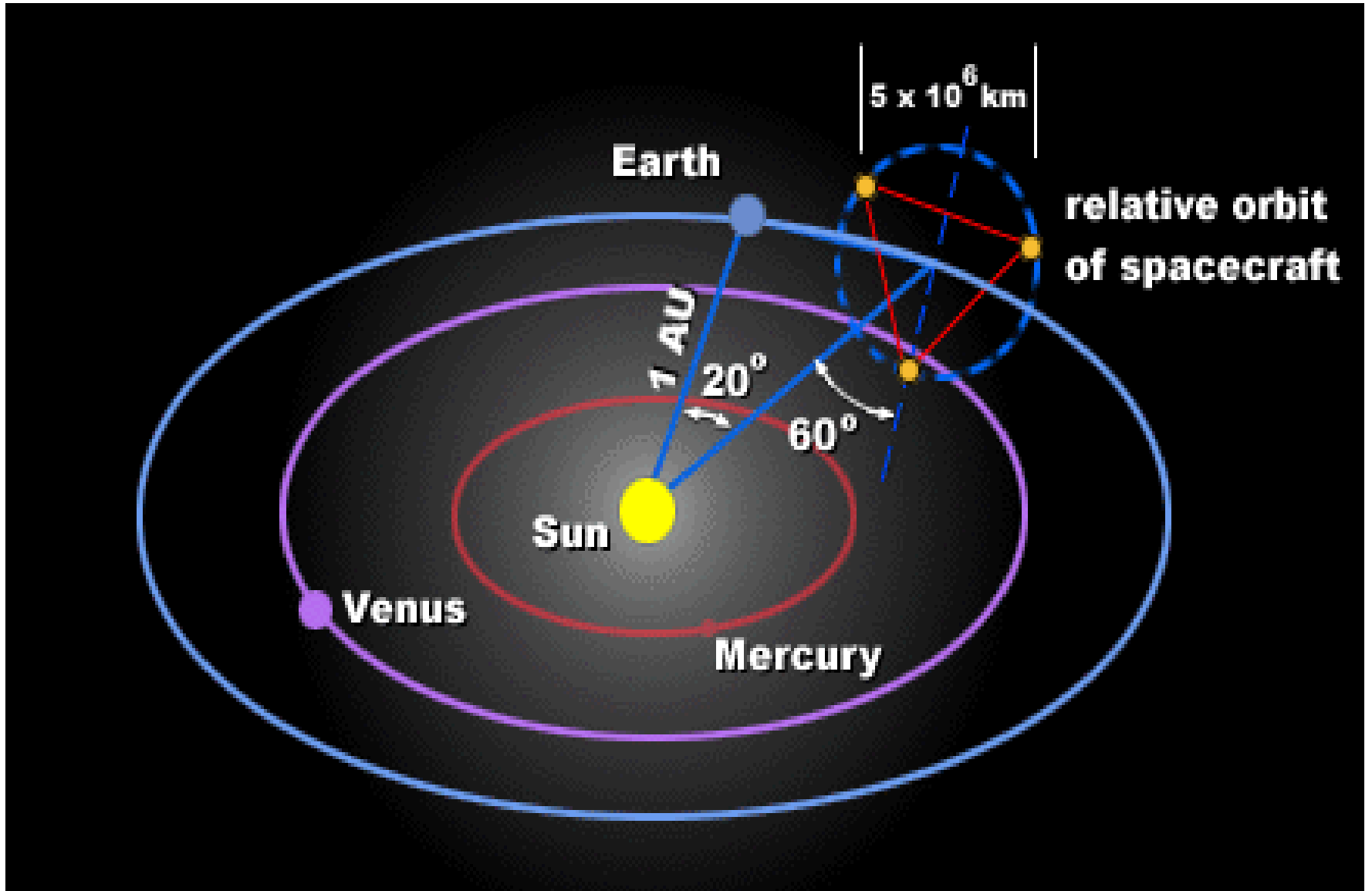
*Jet Propulsion Laboratory,
California Institute of Technology*

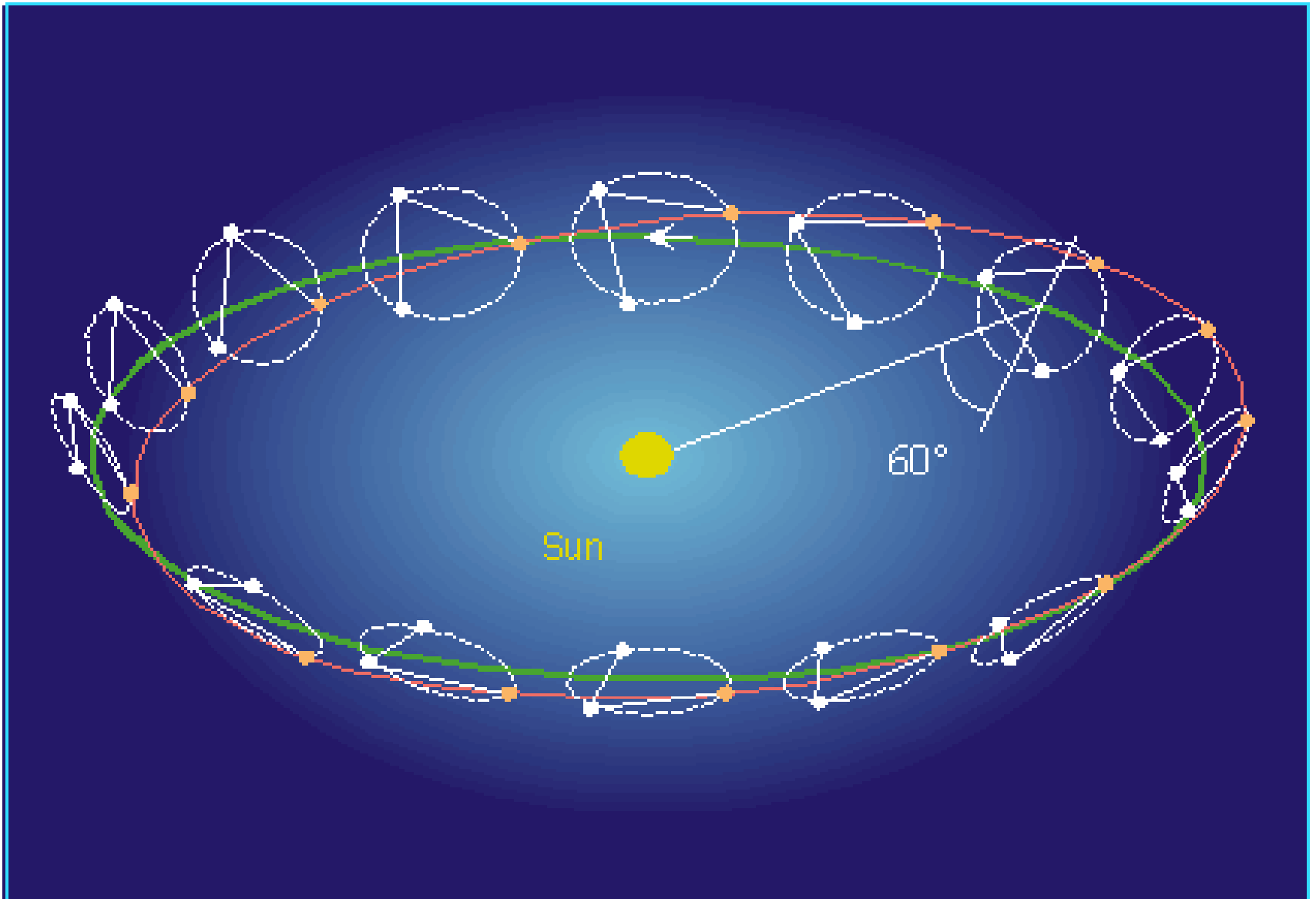


CAJAGWR Seminar – April 5, 2002











What's an Interferometer Detector of Gravitational Waves?

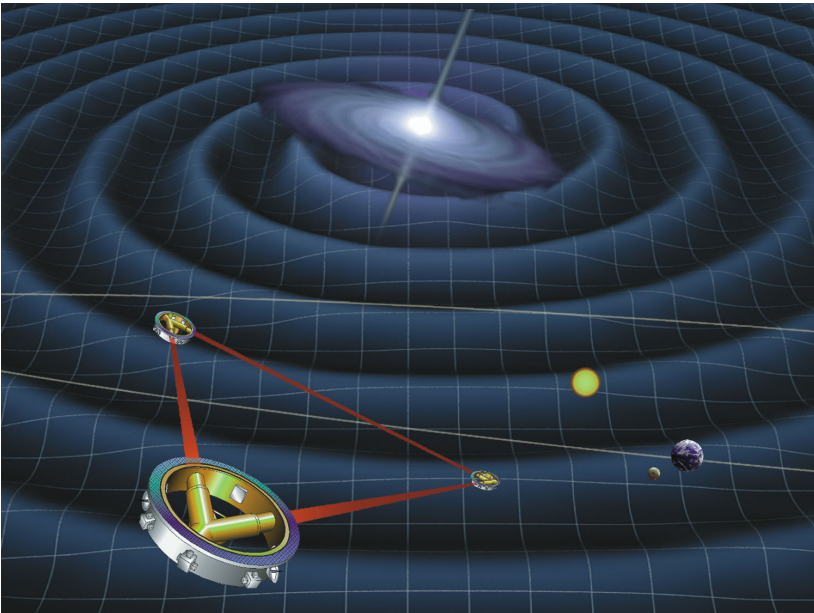


- It is a broad-band instrument that compares phases of split beams propagated along non-parallel arms.
- In so doing, source frequency fluctuations (laser fluctuations) can be removed, and gravitational wave signals at levels many orders of magnitude lower can be detected!

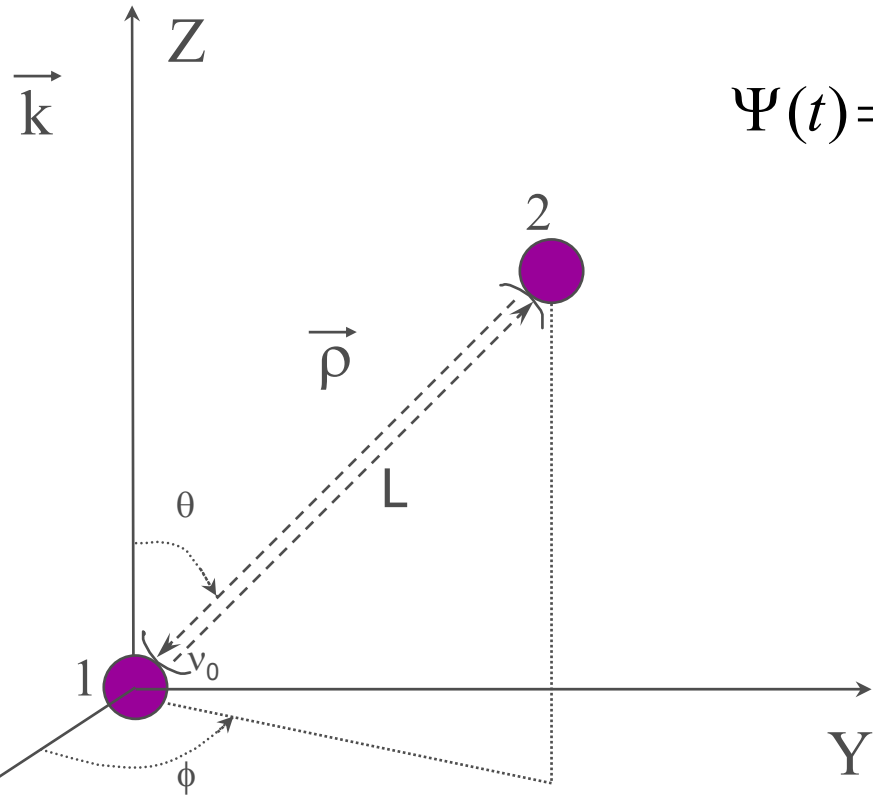
Earth vs. Space-based Interferometers



- Earth-based interferometers have arm lengths essentially equal. This is in order to directly remove laser frequency fluctuations at the photodetector, where the two beams interfere.
- They operate in the long-wavelength limit ($L \ll \lambda$).
- By contrast, LISA will have arm lengths significantly different ($\Delta L/L \sim 10^{-2}$), with $L = 5 \times 10^6$ km.
- Over much of its sensitivity frequency-band, it will **not** operate in the long-wavelength regime.
- Time-of-flight delays in the response to the wave, and travel times along the beams in the detector must be allowed for, in order to derive a correct theory of the detector response.



The Gravitational Wave Signal: The Three-Pulse Response Function



$$\Psi(t) = \frac{\rho^i \rho^j}{2[1 - (\vec{k} \cdot \vec{\rho})^2]} h_{ij}(t)$$

Estabrook, F.B., & Wahlquist, H.D., *Gen.Relativ.Gravit.* 6,439 (1975)

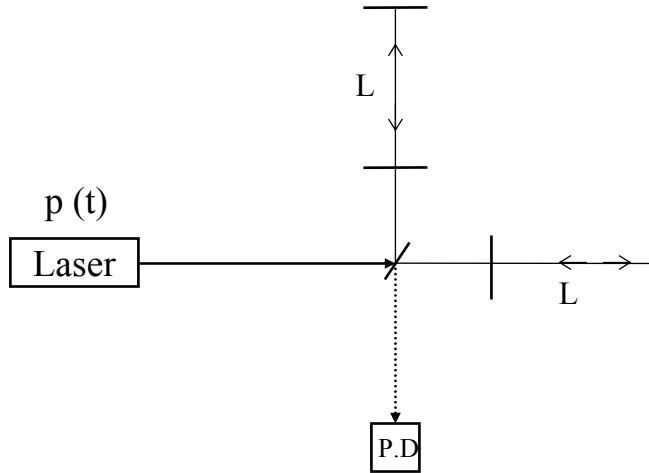
Speed of light = 1

$$\left[\frac{\Delta v(t)}{v_0} \right]_{GW} = -(1 - \vec{k} \cdot \vec{\rho}) \Psi(t) - 2(\vec{k} \cdot \vec{\rho}) \Psi[t - (1 + \vec{k} \cdot \vec{\rho})L] + (1 + \vec{k} \cdot \vec{\rho}) \Psi(t - 2L)$$

Statement of The Problem

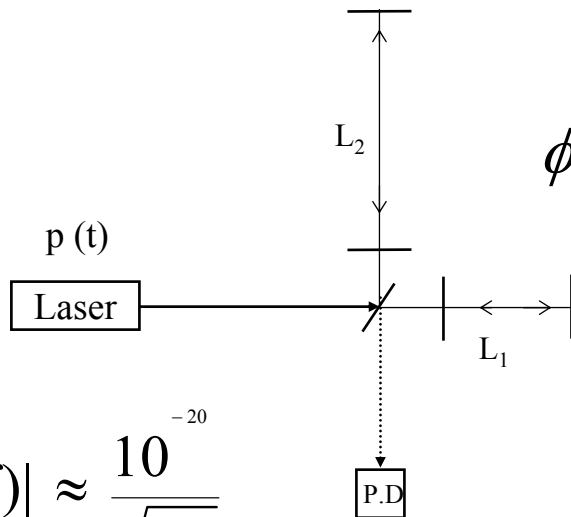
$p(t)$ = Laser phase fluctuations

$$\frac{1}{2\pi\nu_0} \frac{dp(t)}{dt} \equiv \left[\frac{\Delta\nu(t)}{\nu_0} \right]_{\text{Laser}} = C(t)$$



$$\phi_1(t) = h_1(t) + p(t - 2L_1) + n_1(t)$$

$$\phi_2(t) = h_2(t) + p(t - 2L_2) + n_2(t)$$

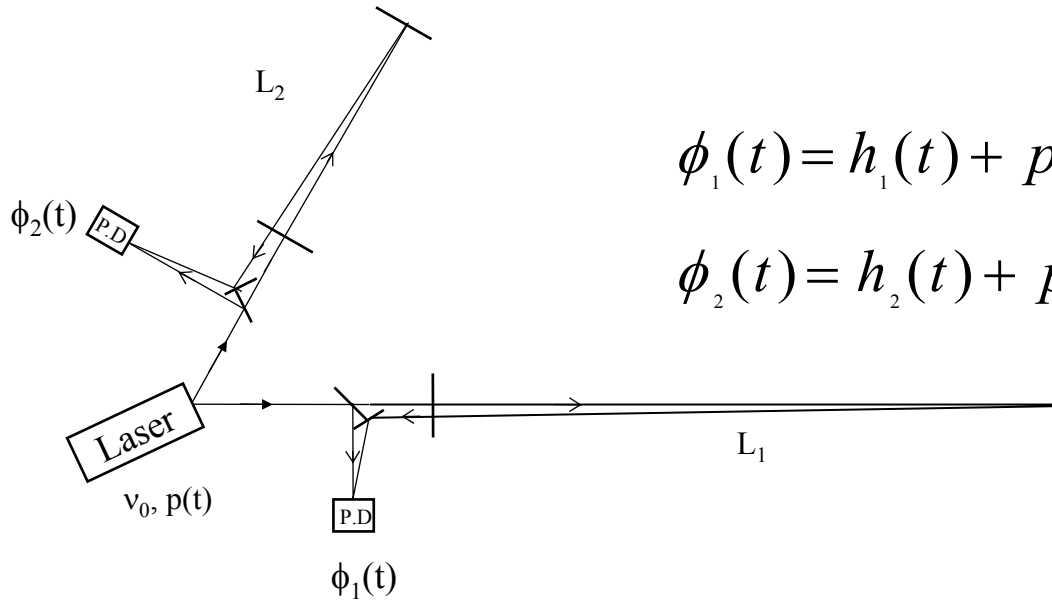


$$\phi_1(t) - \phi_2(t) \Rightarrow p(t - 2L_1) - p(t - 2L_2) \cong 2 \frac{dp}{dt} \varepsilon L_1$$

$$|\tilde{h}(f)| \approx \frac{10^{-20}}{\sqrt{\text{Hz}}}$$

$$|\tilde{C}(f)| \approx \frac{10^{-13}}{\sqrt{\text{Hz}}}, \quad \varepsilon \cong 3 \times 10^{-2} \Rightarrow \frac{5 \times 10^{-16}}{\sqrt{\text{Hz}}}$$

Unequal-arm Interferometers



$$\phi_1(t) = h_1(t) + p(t - 2L_1) - p(t) + n_1(t)$$

$$\phi_2(t) = h_2(t) + p(t - 2L_2) - p(t) + n_2(t)$$

$$\phi_1(t) - \phi_2(t) = h_1(t) - h_2(t) + p(t - 2L_1) - p(t - 2L_2) + n_1(t) - n_2(t)$$

$$\begin{aligned} \phi_1(t - 2L_2) - \phi_2(t - 2L_1) = & h_1(t - 2L_2) - h_2(t - 2L_1) + \\ & p(t - 2L_1) - p(t - 2L_2) + n_1(t - 2L_2) - n_2(t - 2L_1) \end{aligned}$$

$$X(t) \equiv [\phi_1(t) - \phi_2(t)] - [\phi_1(t - 2L_2) - \phi_2(t - 2L_1)]$$

$\phi_1(t)$

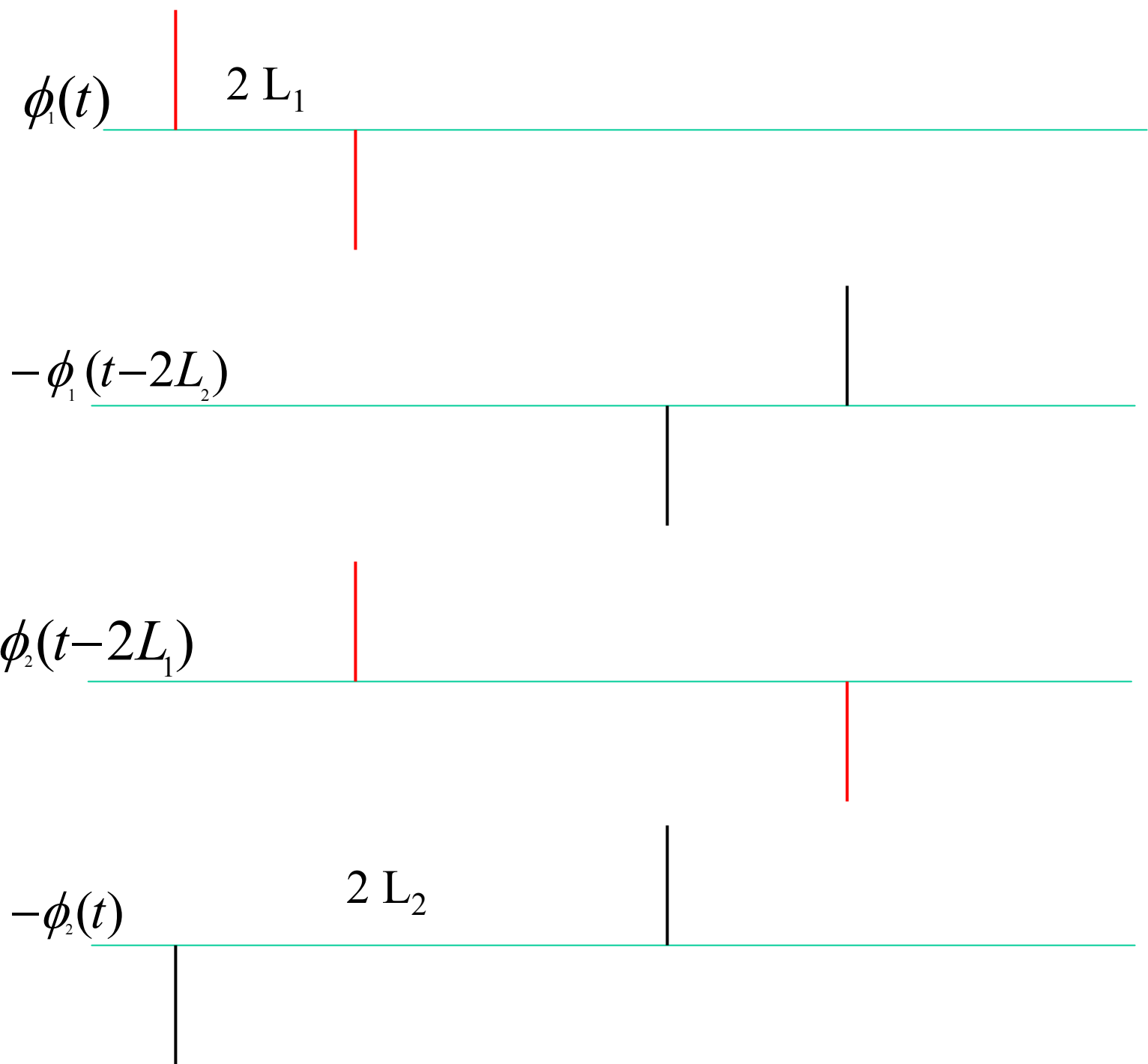
$2 L_1$

$\phi_1(t-2L_2)$

$\phi_2(t-2L_1)$

$\phi_2(t)$

$2 L_2$



Unequal-arm Interferometer (cont.)

- The real limitations on the procedure above come from the remaining noise sources entering the two phase measurements, and the accuracy in the determination of the distances L_1 , L_2 .
- The value of the arm length accuracy required is determined by the magnitude of the phase noise of the laser as well as the noise level determined by the other noise sources entering into $X(t)$.
- Our analysis shows that an arm length accuracy of **30 m** is needed in order to suppress the laser noise below the noise level determined by the other noises entering in $X(t)$.

What is the detector sensitivity?

$$X(t) = [h_1(t) - h_2(t)] - [h_1(t - 2L_2) - h_2(t - 2L_1)] \\ + [n_1(t) - n_2(t)] - [n_1(t - 2L_2) - n_2(t - 2L_1)]$$

$$h_i(t) = -(1 - \vec{k} \cdot \vec{\rho}_i) \Psi_i(t) - 2(\vec{k} \cdot \vec{\rho}_i) \Psi_i[t - (1 + \vec{k} \cdot \vec{\rho}_i)L_i] + (1 + \vec{k} \cdot \vec{\rho}_i) \Psi_i(t - 2L_i)$$

$n_i(t)$ = *Random processes associated with the remaining noises ; i = 1, 2*

In the case of LISA, $L_1 - L_2 \sim 3 \times 10^{-2} L \Rightarrow$

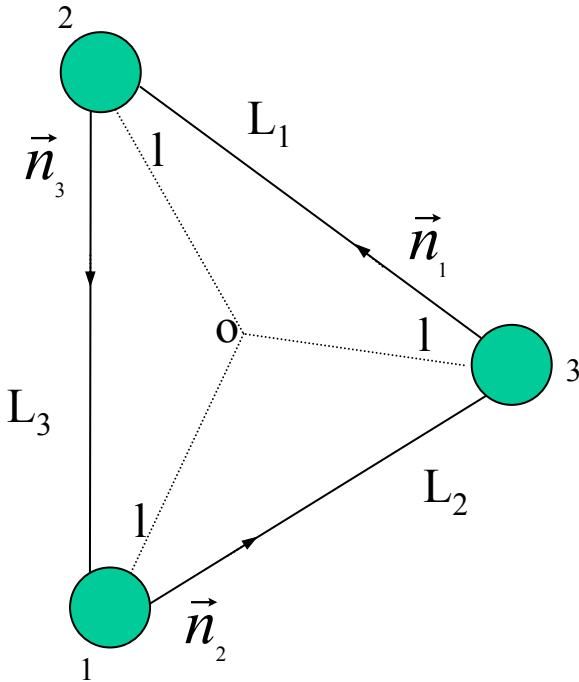
$$X(t) = [h_1(t) - h_2(t)] - [h_1(t - 2L) - h_2(t - 2L)] \\ + [n_1(t) - n_2(t)] - [n_1(t - 2L) - n_2(t - 2L)]$$

$$\tilde{X}(f) = [\tilde{h}_1(f) - \tilde{h}_2(f)][1 - e^{4\pi i f L}] + [\tilde{n}_1(f) - \tilde{n}_2(f)][1 - e^{4\pi i f L}]$$

The SNR of the LISA X-response is the same as the SNR of an equal-arm Michelson.

Time-delay Interferometry

- It is best to think of LISA as a closed array of six one-way delay lines between the test masses.
- This approach allows us to reconstruct the unequal-arm Michelson interferometer, as well as new interferometric combinations, which offer advantages in hardware design, in robustness to failures of single links, and in redundancy of data.



The Two-Way and One-Way Doppler responses

$$\frac{\Delta \nu(t)}{\nu_0} = -(1 - \vec{k} \cdot \vec{n}_3) \Psi_3(t) - 2(\vec{k} \cdot \vec{n}_3) \Psi_3[t - (1 + \vec{k} \cdot \vec{n}_3)L_3] + (1 + \vec{k} \cdot \vec{n}_3) \Psi_3(t - 2L_3) \\ + C_1(t - 2L_3) - C_1(t) + N(t)$$

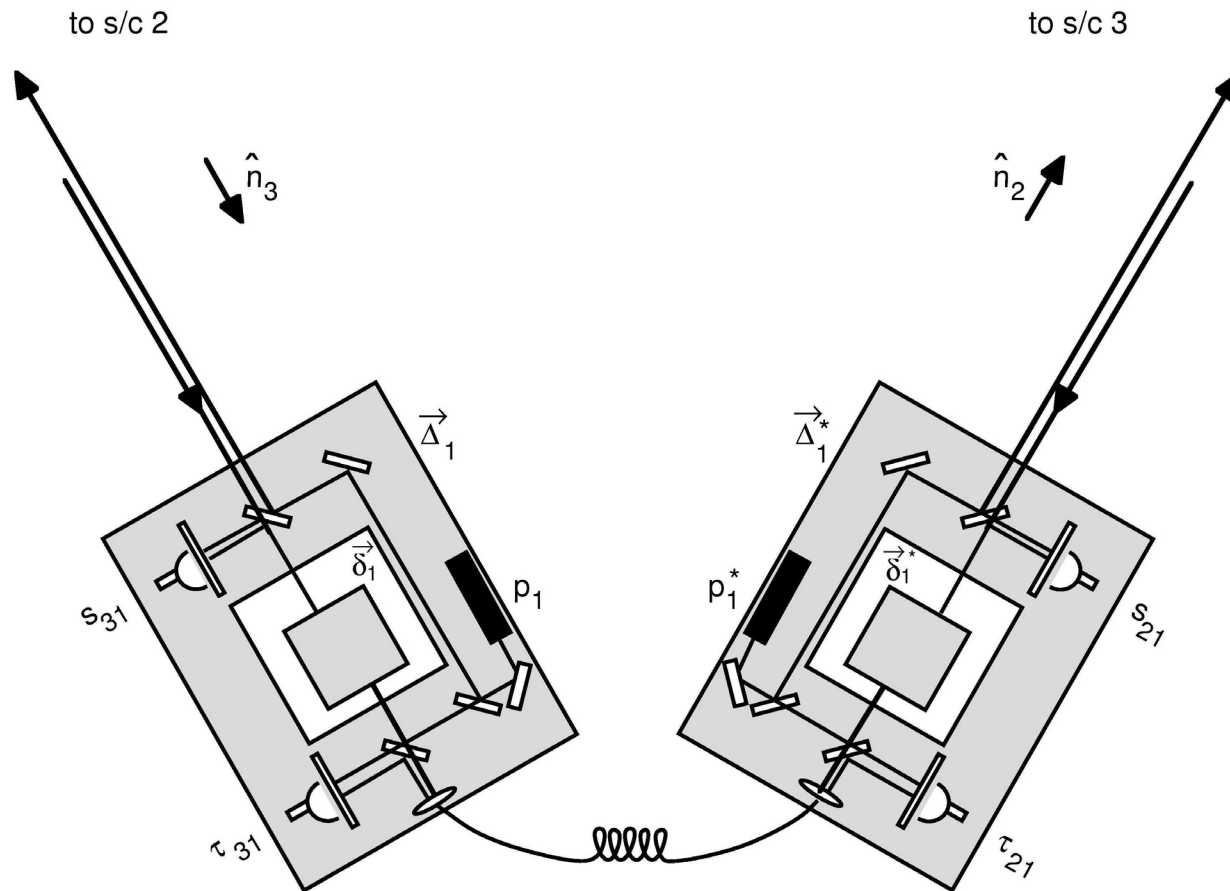
$$\frac{\Delta \nu(t)}{\nu_0} \Big|_{31} = (1 - \vec{k} \cdot \vec{n}_3) [\Psi_3(t - (1 + \vec{k} \cdot \vec{n}_3)L_3) - \Psi_3(t)] + C_2(t - L_3) - C_1(t) + N_{31}(t)$$

$$\frac{\Delta \nu(t)}{\nu_0} \Big|_{32} = (1 + \vec{k} \cdot \vec{n}_3) [\Psi_3(t - L_3) - \Psi_3(t - \vec{k} \cdot \vec{n}_3 L_3)] + C_1(t - L_3) - C_2(t) + N_{32}(t)$$

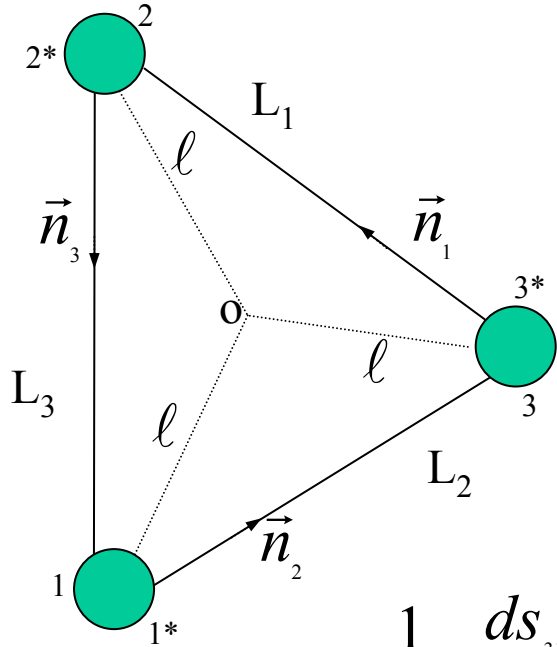
- If we have “sufficient” accuracy in the knowledge of the distance between the two spacecraft (30 m), and the onboard clocks are synchronized (100 ns), we can derive the two-way Doppler data by linearly combining the two one-way measurements:

$$\frac{\Delta \nu(t)}{\nu_0} = \frac{\Delta \nu(t)}{\nu_0} \Big|_{31} + \frac{\Delta \nu(t - L)}{\nu_0} \Big|_{32}$$

Time-delay Interferometry & The Drag-free Configuration



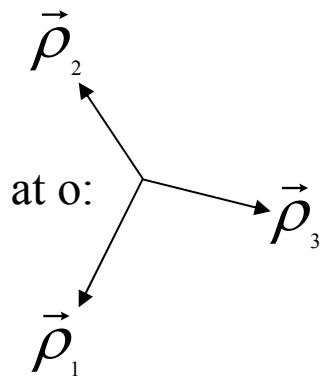
Time-Delay Interferometry.....(cont.)



- $s_{31}(t)$ = phase difference measured at spacecraft # 1, with transmission at spacecraft # 2;
- $s_{21}(t)$ = phase difference measured at spacecraft # 1, with transmission at spacecraft # 3;
- $s_{31,2} = s_{31}(t - L_2)$; all the other one-way responses can be obtained by permutation of the indices.
- The contribution of a GW $h_{ij}(t)$ to the one way responses is given by:

$$\frac{1}{2\pi\nu_0} \frac{ds_{31}(t)}{dt} \Big|_{GW} = \left[1 + \frac{\ell}{L_3} (\mu_1 - \mu_2) \right] [\Psi_3(t - \mu_2 \ell - L_3) - \Psi_3(t - \mu_1 \ell)]$$

$$\frac{1}{2\pi\nu_0} \frac{ds_{21}(t)}{dt} \Big|_{GW} = \left[1 - \frac{\ell}{L_2} (\mu_3 - \mu_1) \right] [\Psi_2(t - \mu_3 \ell - L_2) - \Psi_2(t - \mu_1 \ell)]$$



$$\mu_i = \vec{k} \cdot \vec{\rho}_i$$

$$\Psi_i(t) = \frac{\vec{n}_i \cdot \vec{h}(t) \cdot \vec{n}_i}{2[1 - (\vec{k} \cdot \vec{n}_i)^2]}$$

Twelve One-way Measurements!

$$s_{21} = s_{21}^{GW} + p_{3,2} - p_{1}^* - \nu_0 \vec{n}_2 \cdot \vec{\Delta}_{3,2} + \nu_0 \vec{n}_2 \cdot [2\vec{\delta}_1^* - \vec{\Delta}_1^*] + s_{21}^{shot}$$

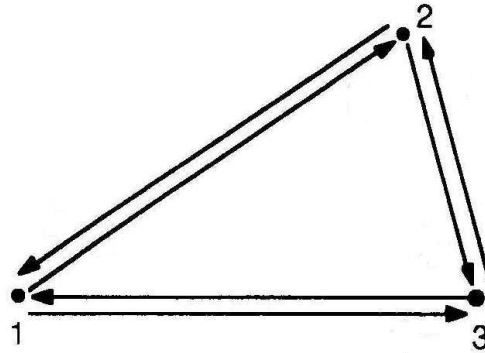
$$\tau_{21} = p_1 - p_{1}^* + 2\nu_0 \vec{n}_3 \cdot [\vec{\delta}_1 - \vec{\Delta}_1] + \mu_1$$

$$s_{31} = s_{31}^{GW} + p_{2,3}^* - p_1 + \nu_0 \vec{n}_3 \cdot \vec{\Delta}_{2,3}^* + \nu_0 \vec{n}_3 \cdot [-2\vec{\delta}_1 + \vec{\Delta}_1] + s_{31}^{shot}$$

$$\tau_{31} = p_{1}^* - p_1 - 2\nu_0 \vec{n}_3 \cdot [\vec{\delta}_1^* - \vec{\Delta}_1^*] + \mu_1$$

- Eight other relations are obtained by cyclic permutation of the indices in the equations above.

Six-Pulse Data Combinations



$\alpha, \beta, \gamma, \zeta$

Data Combinations That Eliminate Laser Noise and Optical Bench Motions

- Unequal-arm Sagnac: α, β, γ

$$\alpha = S_{21} - S_{31} + S_{13,2} - S_{12,3} + S_{32,12} - S_{23,13}$$

$$- \frac{1}{2} (\tau_{13,2} + \tau_{13,13} + \tau_{21} + \tau_{21,123} + \tau_{32,3} + \tau_{32,12})$$

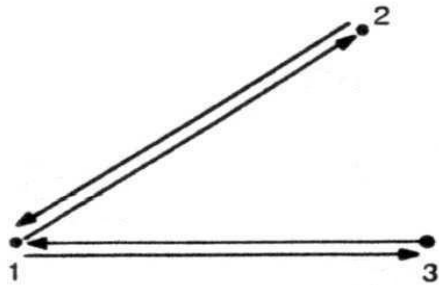
$$+ \frac{1}{2} (\tau_{23,2} + \tau_{23,13} + \tau_{31} + \tau_{31,123} + \tau_{12,3} + \tau_{12,12})$$

Data Combinations that...(cont.)

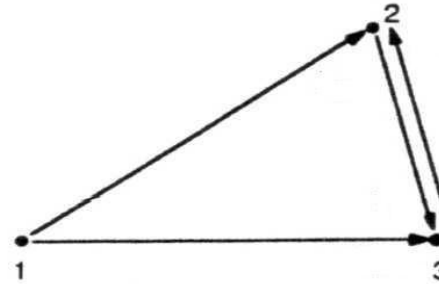
- Unequal-arm Symmetrized Sagnac : ζ

$$\begin{aligned} \zeta = & S_{32,2} - S_{23,3} + S_{13,3} - S_{31,1} + S_{21,1} - S_{12,2} \\ & + \frac{1}{2} (-\tau_{13,21} + \tau_{23,12} - \tau_{21,23} + \tau_{31,23} - \tau_{32,13} + \tau_{12,13}) \\ & + \frac{1}{2} (-\tau_{32,2} + \tau_{12,2} - \tau_{13,3} + \tau_{23,3} - \tau_{21,1} + \tau_{31,1}) \end{aligned}$$

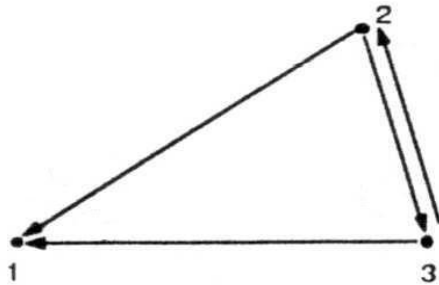
Eight-Pulse Data Combinations



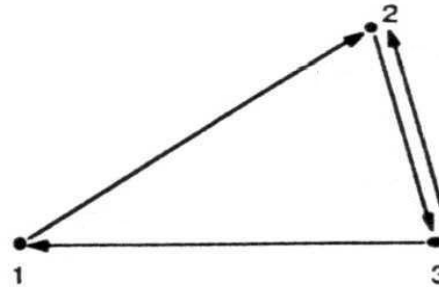
INTERFEROMETER (X,Y,Z)



BEACON (P,Q,R)



MONITOR (E,F,G)



RELAY (U,V,W)

Data Combinations (cont.)

- Unequal-arm Michelson : X, Y, Z

$$\begin{aligned}
 X = & s_{32,322} - s_{23,233} + s_{31,22} - s_{21,33} + s_{23,2} - s_{32,3} + s_{21} - s_{31} \\
 & + \frac{1}{2}(-\tau_{21,2233} + \tau_{21,33} + \tau_{21,22} - \tau_{21}) \\
 & + \frac{1}{2}(\tau_{31,2233} - \tau_{31,33} - \tau_{31,22} + \tau_{31})
 \end{aligned}$$

Data Combinations (cont.)

- Unequal-arm Beacon response: P, Q, R

$$P = \zeta - \alpha_{,1}$$

- Unequal-arm Monitor response: E, F, G

$$E = \alpha - \zeta_{,1}$$

Data Combinations (cont.)

- Unequal-arm Relay response: U, V, W

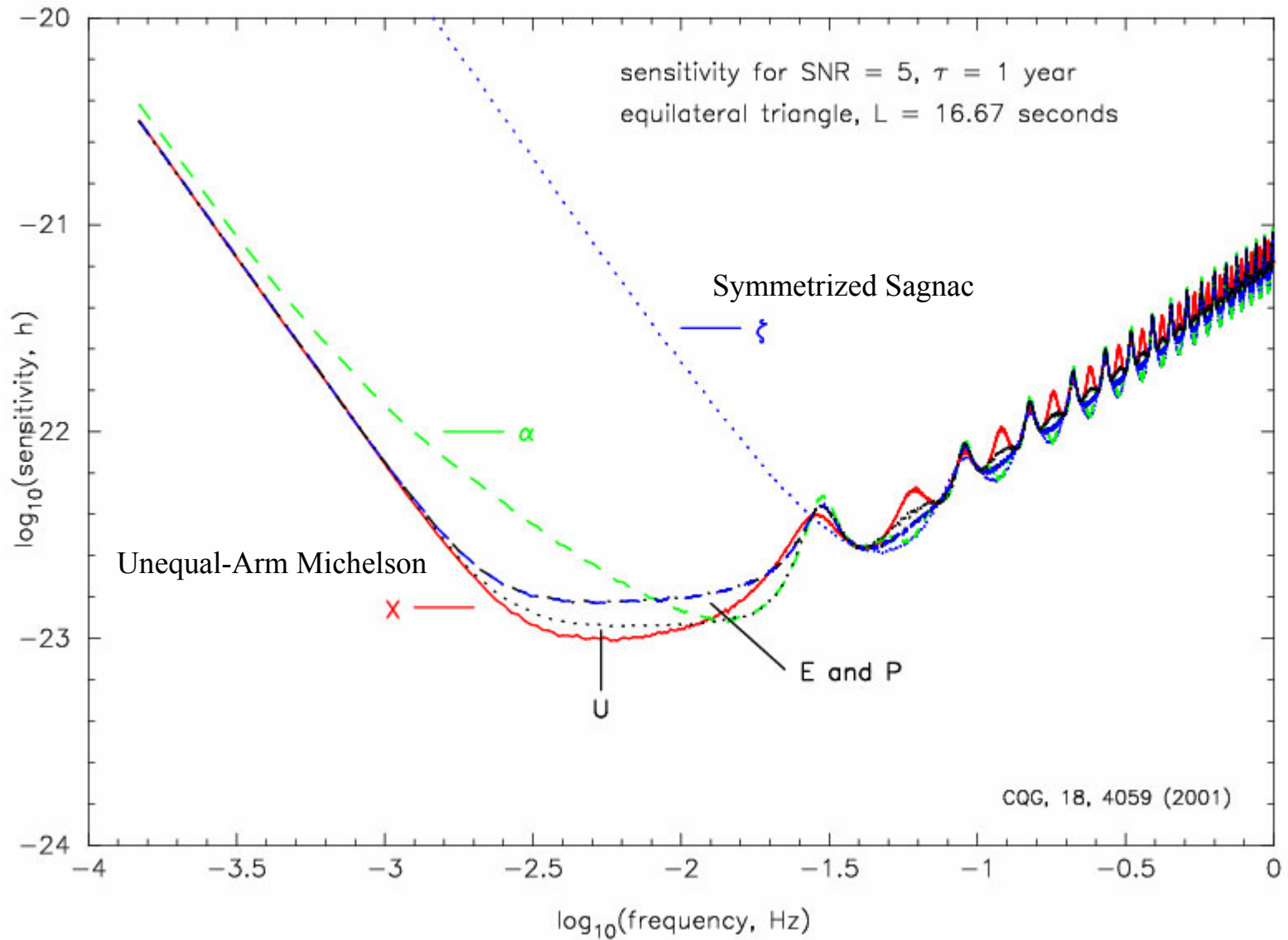
$$U = \gamma_1 - \beta$$

- The expressions above are free from the six phase noises from the lasers, as well as the six phase fluctuations introduced by the motion of the optical benches.

Data Combinations (cont)

- In summary: there are 6 optical benches, 6 lasers, and a total of 12 Doppler time series observed.
- The 6 beams exchanged between distant spacecraft contain the information about the GW signal (s_{ij}); the other 6 signals (τ_{ij}) are for comparison of the lasers and relative optical bench motions within the spacecraft.
- The functional space of interferometric combinations is 3-dimensional.

$$\begin{aligned} \zeta - \zeta_{,123} &= \alpha_{,1} - \alpha_{,23} + \beta_{,2} - \beta_{,31} + \gamma_{,3} - \gamma_{,12} \\ X_{,1} &= \alpha_{,32} - \beta_{,2} - \gamma_{,3} + \zeta \\ Y_{,2} &= \beta_{,13} - \gamma_{,3} - \alpha_{,1} + \zeta \\ Z_{,3} &= \gamma_{,21} - \alpha_{,1} - \beta_{,2} + \zeta \end{aligned}$$



The Laser Frequencies Are Different, and the Spacecraft Are Not Stationary

- As a consequence of having lasers with different frequencies, the phase noise due to the vibrations of the optical benches will no longer cancel out exactly in the laser-noise-free data combinations.
- Both frequency offsets between lasers, and Doppler drifts, now bring in noise from the onboard oscillators (USO=Ultra Stable Oscillators) used in the down-conversion of phototube fringe rates.
- A state-of-the-art USO with a frequency stability of $\sim 10^{-13}$ in the millihertz band will introduce relative frequency fluctuations in the interferometric data equal to 3.0×10^{-20} (1 year integration, 5σ level).

One-way Responses

$$s_{21} = [\nu_3(1 - \dot{L}_2) - \nu^*_1 - a_{21} f_1]t + p_{3,2} - p^*_{1,1} - a_{21} q_1 - \nu_3 \vec{n}_2 \cdot \vec{\Delta}_{3,2} \\ + \nu_3(1 - \dot{L}_2) \vec{n}_2 \cdot [2\vec{\delta}_1^* - \vec{\Delta}_1^*] + s_{21}^{GW} + s_{21}^{shot}$$

$$\tau_{21} = [\nu_1 - \nu^*_1 - c_{21} f_1]t + p_1 - p^*_{1,1} - c_{21} q_1 + 2\nu_1 \vec{n}_3 \cdot [\vec{\delta}_1 - \vec{\Delta}_1] + \mu_1$$

$$s_{31} = [\nu^*_2(1 - \dot{L}_3) - \nu_1 - a_{31} f_1]t + p^*_{2,3} - p_1 - a_{31} q_1 + \nu^*_2 \vec{n}_3 \cdot \vec{\Delta}_{2,3}^* \\ + \nu^*_2(1 - \dot{L}_3) \vec{n}_3 \cdot [-2\vec{\delta}_1 + \vec{\Delta}_1] + s_{31}^{GW} + s_{31}^{shot}$$

$$\tau_{31} = [\nu^*_1 - \nu_1 - c_{31} f_1]t + p^*_{1,1} - p_1 - c_{31} q_1 - 2\nu^*_1 \vec{n}_2 \cdot [\vec{\delta}_1^* - \vec{\Delta}_1^*] + \mu_1$$

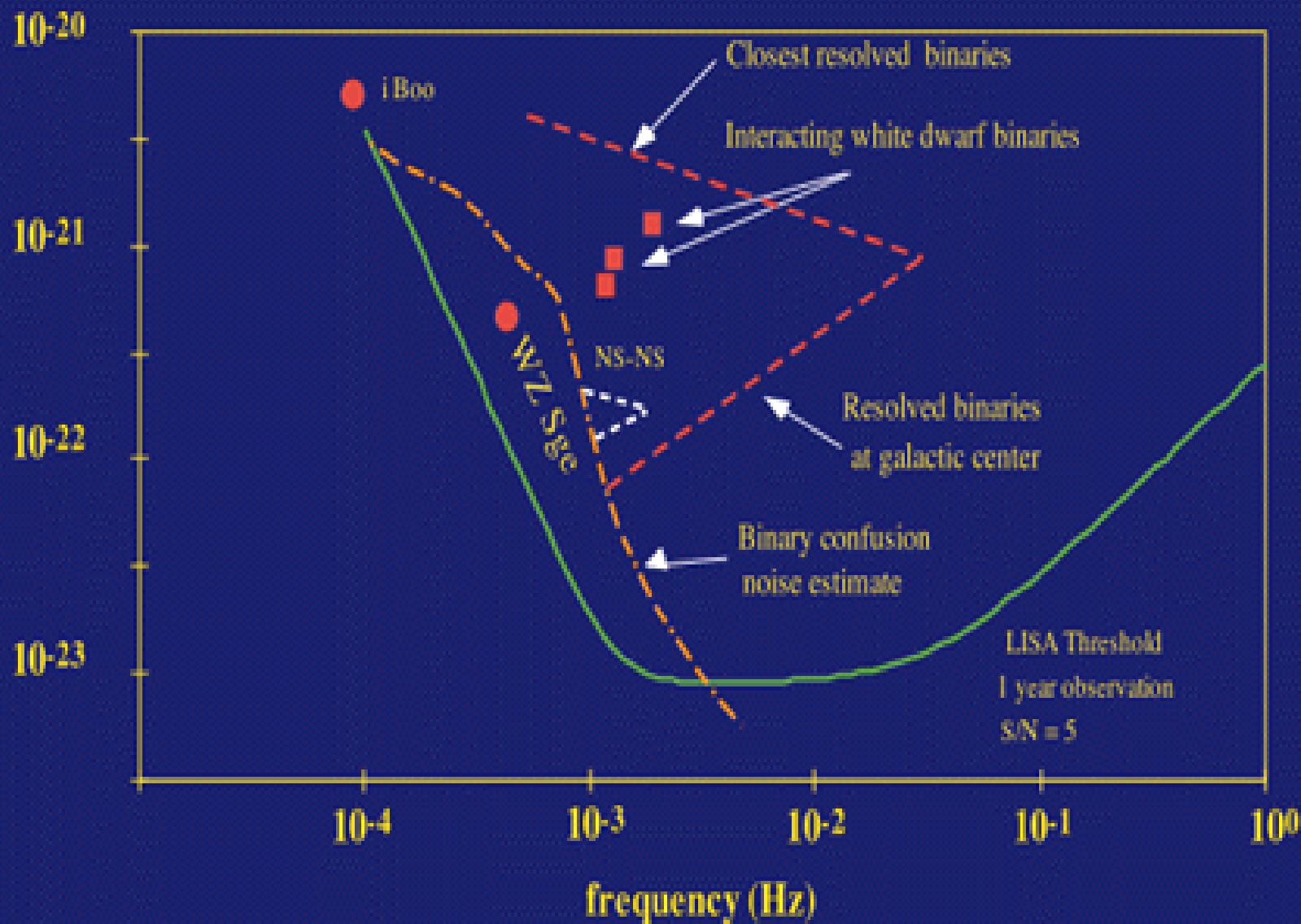
$$a_{21} = \frac{\nu_3(1 - \dot{L}_2) - \nu^*_1}{f_1} \quad ; \quad a_{31} = \frac{\nu^*_2(1 - \dot{L}_3) - \nu_1}{f_1} \quad ; \quad c_{31} = -c_{21} = \frac{\nu^*_1 - \nu_1}{f_1}$$

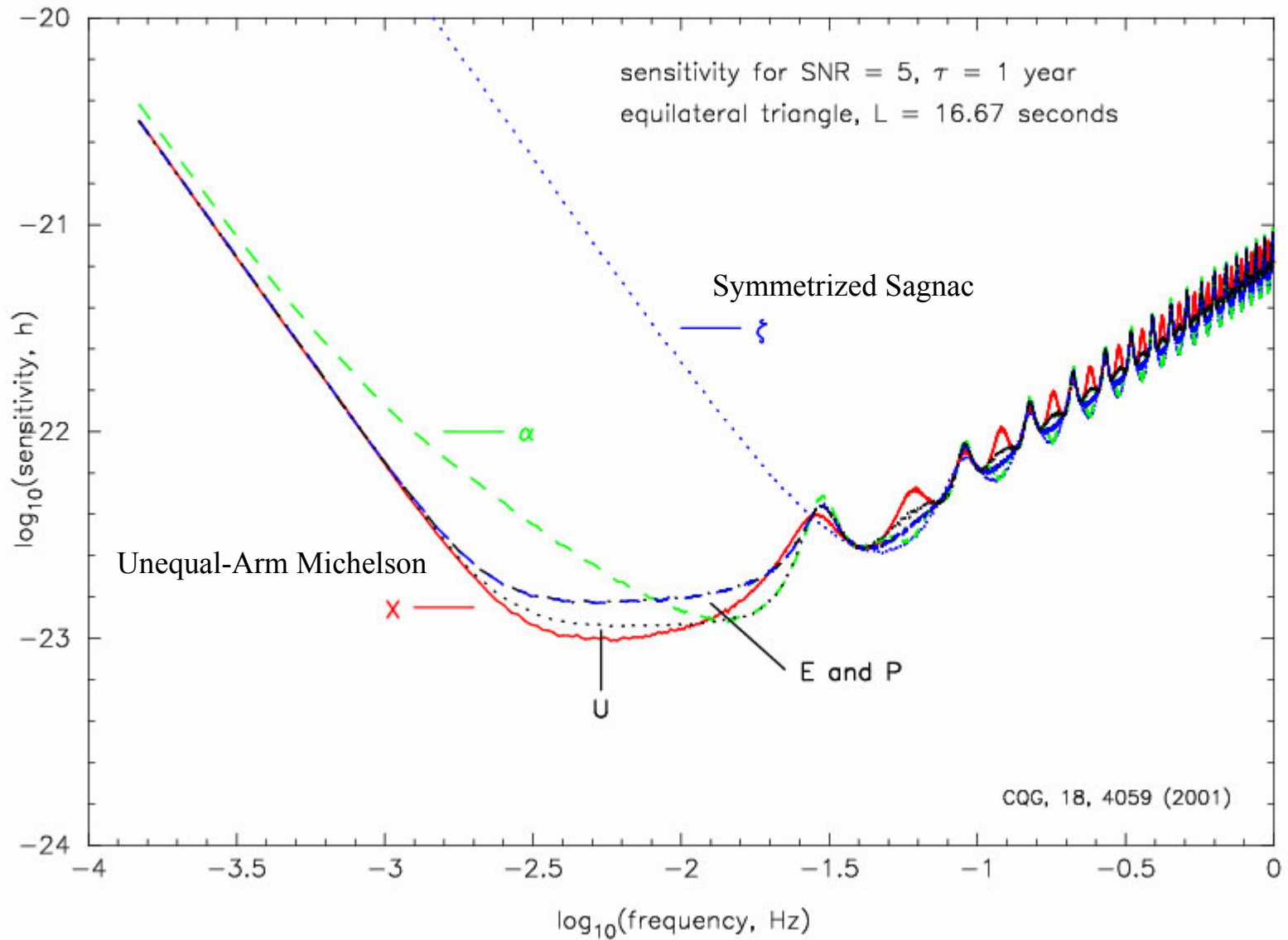
- $(f_i, q_i; i=1, 2, 3)$ are the frequencies and phase noises of the 3 USOs respectively

One-way Responses (cont.)

- In the scheme first proposed by Hellings, Danzmann *et al.* (Optics Comm., **124**, 313, 1996) , in addition to the six main laser signals of frequencies ν_i , ν_i^* , a second laser signal is superimposed on each beam by either modulating it at the frequency f_i of its USO (two side-bands), or by combining each beam with a coherent second signal at $\nu_i + f_i$ or $\nu_i^* + f_i$
- The transmitted second signals are heterodyned against the local second signal, and independently down converted with coefficients, say b_{ij} (different from the a_{ij} introduced earlier!) to give six additional data records, s'_{ij}
- By introducing the observables $r_{ij} = s_{ij} - s'_{ij}$, USO phase noise can be measured and calibrated-out from the interferometric combinations.

Strain amplitude h

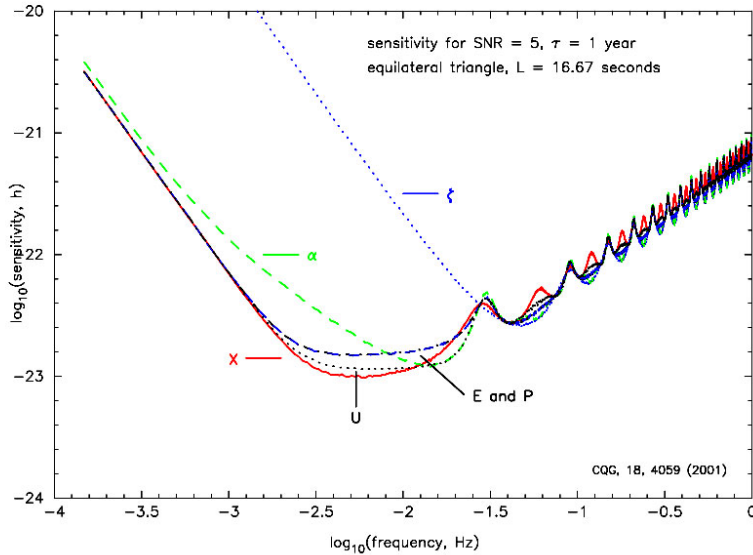




NOISE CALIBRATION and DETECTION OF A STOCHASTIC BACKGROUND

- The gravitational wave background will be below the anticipated sensitivity curve of ζ by several orders of magnitude.
- The Sagnac combination provides a way for estimating the instrumental noise sources: Sagnac greatly attenuates the gravitational wave signal, but instrumental noise persists.
- This allows us to infer the actual on-orbit LISA instrumental noise in the Michelson interferometer mode X, and in turn to detect the stochastic background (M. Tinto, J.W. Armstrong, & F.B. Estabrook, *Phys. Rev. D*, **63**, 021101(R) (2001)).
- The ζ combination can of course be used also as a discriminator for sinusoidal signals and bursts.
- Hogan and Bender (*Phys. Rev. D*, **64**, 062002, 2001) have proposed a technique for improving the LISA sensitivity to backgrounds by properly combining the spectra of ζ , X, Y, and Z.

Optimal Interferometric Combinations



- Q: Is there a systematic way to derive another set of interferometric combinations that show “optimal” sensitivity?
- A: YES!

$$SNR^2 = \int \frac{|a_1(f)\tilde{X}_s + a_2(f)\tilde{Y}_s + a_3(f)\tilde{Z}_s|^2}{\langle |a_1(f)\tilde{X}_n + a_2(f)\tilde{Y}_n + a_3(f)\tilde{Z}_n|^2 \rangle} df$$

- One should regard the SNR as a functional of the functions $a_i(f)$, and extremize it with respect of them.

Conclusions

- T.D.I. provides an exact method for canceling the leading noise source – laser phase fluctuations – in an interferometer with unequal, time-variable arms.
- It relies on specific use of time-delays between the LISA spacecraft.
- It allows analysis of signals, noises, achievable sensitivities, and architectural design (including system-level tradeoffs between, e.g. laser stability, arm length accuracy, stability of optical bench, Doppler shifts due to chosen orbits, USO stability).
- It provides robustness of the mission with respect to failures of subsystems.
- It shows existence of alternate LISA configurations offering potential design, implementation, or cost advantages.
- It gives a data combination (ζ) for assessing the LISA on-orbit instrumental noise performance.